J Gastroenterol 1996; 31:46–54

Journal of Gastroenterology

Immunohistochemical study of proteoglycans in D-galactosamine-induced acute liver injury in rats

SHUNSUKE SASAKI, NORIO KOIDE, TOSHIYUKI SHINJI, and TAKAO TSUJI

First Department of Internal Medicine, Okayama University Medical School, 2-1-5 Shikata-cho, Okayama, 700 Japan

Abstract: In this study, we carried out an immunohistochemical investigation of time-dependent alterations in the distribution of proteoglycans, and the proliferation profiles of hepatocytes and fat-storing cells (FSCs) in the livers of rats intoxicated with D-galactosamine (GalN). The proliferative cells were analyzed by proliferative cell nuclear antigen (PCNA) staining. In untreated rats, heparan sulfate, dermatan sulfate, and chondroitin/chondroitin sulfate were detected within the portal spaces and the central veins, and, with the exception of chondroitin, also within the reticular fibers. After administration of GalN, the number of PCNA-positive cells (FSCs and hepatocytes) and FSCs increased, reaching maximal on the 2nd and 3rd days, respectively. Heparan sulfate showed complicated changes. Dermatan sulfate decreased in portal spaces from the 2nd to the 3rd day, and in reticular fibers from 12 h to the 6th day. Chondroitin/chondroitin sulfate staining was observed from 2 h to the 6th day in the sinusoidal endothelia, which suggests that the sinusoidal endothelia may produce chondroitin/chondroitin sulfate transiently during liver damage as part of the mechanism of regeneration. Heparan sulfate and chondroitin/chondroitin sulfate were detected in necrotic regions, but dermatan sulfate was not. These observations suggest that heparan sulfate and chondroitin/chondroitin sulfate are involved in cell proliferation or morphogenesis and that the dermatan sulfate plays a role in the differentiation or functional maintenance of cells in liver regeneration.

Key words: extracellular matrix, D-galactosamine hydrochloride, heparan sulfate, dermatan sulfate, chondroitin/chondroitin sulfate

Offprint requests to: S. Sasaki

(Received for publication on Dec. 15, 1994; accepted on Apr. 28, 1995)

Introduction

The extracellular matrix (ECM) of human and animal liver contains several types of collagens, glycoproteins, proteoglycans (PGs), and elastin as the major classes of components. The ECM provides cohesiveness within tissue compartments, induces polarization of cells, and acts as a major determinant of gene expression and differentiation.[1] Although the ECM is only a small component (by weight) of the liver, it has a crucial role, not only in providing a structural framework, but also in maintaining the differentiated state of hepatocytes.[2] This role of the hepatic matrix has been clearly demonstrated in cell culture, where the hepatocyte phenotype has been shown to be dramatically altered, dependent on the nature of the matrix substratum upon which the cells are cultured.[3] The hepatic ECM undergoes quantitative and qualitative changes in pathological states.[4,5] Until now, however, no data have been available concerning the time-dependent changes of the histological expression of PGs in acute liver injury. In this study, using an immunohistochemical method, we examined the time-dependent changes in hepatic proteoglycans, in addition to such changes in proliferating FSCs and hepatocytes, in rats with acute hepatitis induced by D-galactosamine (GalN).

Materials and methods

D-Galactosamine-induced acute liver injury in rats

A total of 190 male Sprague-Dawley rats (Charles River Japan, Yokohama), weighing around 200 g, received a single intraperitoneal injection of GalN (Sigma Chemical Co., St. Louis, Mo.), at 2 g/kg body weight, dissolved in saline (1 g/5 ml) and pH-adjusted to 7.0. Twenty-six untreated rats served as controls.

Four or five GalN-treated rats and two controls were killed at each of the following time points: 2, 6, and 12 h; 1, 2, 3, 4, 5, and 6 days; and 1, 4, 8, and 12 weeks after treatment. A total of 133 rats died spontaneously after GalN injection. Liver samples and sera were processed for biochemical, histological, immunohistochemical, and ultrastructual studies. Serum AST and ALT levels were determined by an enzymatic method, using a biochemical analyzer (TBA-400; Toshiba Co. Ltd., Tokyo, Japan).

Primary antibodies

Monoclonal mouse anti-human dermatan sulfate proteoglycan (6B6), anti-heparan sulfate (HepSS-1), anti-proteoglycan ΔDi-0S (1B5), anti-proteoglycan ΔDi-4S (2B6), and anti-proteoglycan ΔDi-6S (3B3) antibodies were purchased from Seikagaku Kogyo Co. Ltd. (Tokyo, Japan). The characteristics of these antibodies are: HepSS-1 recognizes an epitope present in heparan sulfate (HS);[6] 6B6 recognizes a core peptide, the antigenic properties of which are similar to those of PGII/decorin;[7,8] and 1B5, 2B6, and 3B3 recognize chondroitin (C-0S), chondroitin 4-sulfate (C-4S), and/or dermatan sulfate (DS), as well as chondroitin 6-sulfate (C-6S) stub, with chondroitinase ABC pretreatment.[9] Monoclonal mouse anti-desmin (DE-B-5) and anti-PCNA (PC10) antibodies were obtained from Boehringer Mannheim GmbH (Mannheim, Germany) and Dakopatts (Glostrup, Denmark), respectively.

Immunohistochemical staining for light microscopy (LM)

For routine histological examinations, sections were stained with hematoxylin and eosin (H&E), Azan, periodic acid Schiff (PAS), PAS after diastase digestion, and silver impregnation. For immunohistological studies, tissue blocks were mounted in Tissue-Tek (Miles Laboratories Inc., Elkhart, Ind.), and frozen rapidly in dry ice-ethanol, after which cryostat sections, 3-μm-thick, were cut. The sections were air-dried for 30 min, fixed in acetone for 10 min at −20°C, incubated for 25 min with 0.3% H_2O_2 in methanol, digested for 60 min at room temperature with 0.2 U/ml of chondroitinase ABC (Seikagaku Kogyo Co. Ltd.) in 20 mM Tris-HCl buffer, pH 8.0, washed in PBS, incubated for 20 min with 1% normal goat serum (NGS) and then incubated overnight at 4°C with primary antibodies diluted in PBS, pH 7.4, containing 1% NGS. The reacted primary antibodies were visualized with 0.6 mM 3,3′-diaminobenzidine tetrahydrochloride (DAB)/0.005% H_2O_2 solution, using a Vectastain ABC Elite kit (Vector Laboratories Inc., Burlingame, Calif.) according to the manufacturer's directions, and counterstained with Mayer's hematoxylin. For double-staining with the first primary antibodies and with the second primary antidodies, after the first antibodies were visualized with DAB/H_2O_2 substrate solution, the sections were washed, with continuous stirring, for 2 h in 0.1 M glycine hydrochloride buffer, pH 2.0, and then in PBS. The same procedure as above was then employed with the second antibodies, and the sections were immersed for 5 min in 50 mM Tris-HCl buffer, pH 7.6, containing 1.2 mM 4-methoxy-1-naphthol (Aldrich Chemical Co. Inc., St. Louis, Mo.) and 0.005% H_2O_2, after which they were counterstained with Mayer's hematoxlin and mounted in glycerin-PBS.

Immunohistochemical staining for transmission electron microscopy (TEM)

Tissue blocks were fixed in periodate lysine paraformaldehyde fixative for 24 h, and cut at a thickness of 40 μm with a microslicer. The sections were digested with chondroitinase ABC, incubated with primary antibodies for 24 h, with biotinylated secondary antibodies for 1 h, and with ABC reagent for 1 h. After preincubation in DAB without H_2O_2 for 30 min, the sections were incubated in DAB/H_2O_2 substrate solution for 25 min, postfixed in 2.5% glutaraldehyde for 10 min and in 1% O_sO_4 dissolved in 0.2 M phosphate buffer for 15 min. Ultrathin sections were viewed, either unstained or after staining with lead citrate for 3 min, with a Hitachi H700 electron microscope.

Analytical procedure

The extent of immunoreactivity of individual ECM constituents was graded semiquantitatively on a 0–4 scale (0, absent; 1, trace; 2, weak; 3, moderate; 4, strong), and at least three sections from different rats killed at each time point were examined. The numbers of desmin-positive FSCs and PCNA-positive cells were counted with a LM, at a magnification of 400, with a field measuring 0.1964 mm^2. Three rats were examined at each time point, and one rat served for three sections in the counting of FSCs and for one section in the counting of PCNA-positive cells. In each section, only the number of cells containing a nucleus in the plane was counted in three periportal and three pericentral areas chosen at random. The entire surface area of the microscopic field was regarded as the reference surface area of each microscopic field.

Statistical analysis

The data were expressed as means ± (SD). Statistical significance was analyzed by the two-tailed Mann-Whitney test. When the associated probability was $P < 0.05$, differences were considered significant.

Results

Histological changes

Serum ALT levels increased immediately after GalN injection, reached a peak at 24 h, and decreased to control level after the 6th day (Fig. 1). In H&E-stained and silver-impregnated sections, some reticular fibers in lobules had become slender as early as 2 h after GalN injection. At 12 h, foci of hepatocellular necrosis were disseminated throughout the lobules, and reticular fibers were altered, showing an irregular diameter, and were fragmentary within necrotic areas. From the 1st to 2nd day, reticular fibers disappeared within necrotic areas, and at the same time, bundles of fine and tortuous fibers surrounded proliferative bile ductules or liver cell rosettes around the portal tracts. On the 3rd day, these bundles grew in diameter and expanded around the juvenile hepatocytes, and fine fiber frameworks emerged along with the sinusoids (Fig. 2A–D). Rat livers showed parenchymal necrosis of varying severity, from focal to panacinar necrosis. Histological features in H&E-stained sections returned to normal at 1 week, and the configuration of reticular fibers with silver impregnation returned to normal as late as 12 weeks after GalN administration.

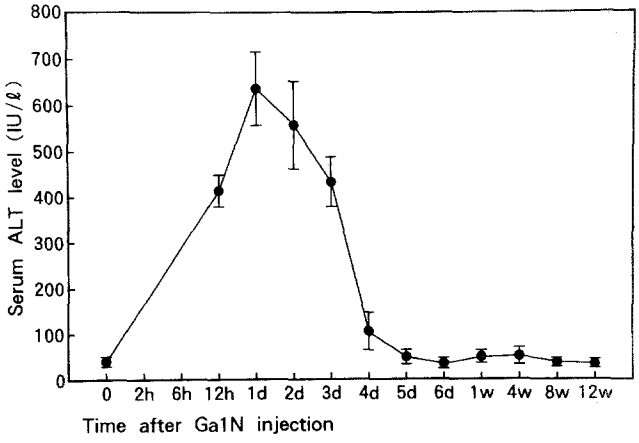

Fig. 1. Changes in serum ALT levels after D-galactosamine (*GalN*) injection. Peak value was observed on the 1st day after GalN injection. The data points represent the mean number of serum ALT levels of three rats at each of the investigated time points. *Vertical bars* represent SD. *h*, hour; *d*, day; *w*, week

Proliferation of hepatocytes and fat-storing cells

Figure 3A summarizes the results for the counting of FSCs. In counting the number of FSCs, we omitted desmin-positive smooth muscle cells and fibroblast-like cells in the portal tracts and central veins.[10,11] The number of FSCs in control rats was 14.0 ± 2.5 cells/0.2 mm^2 in the periportal areas (zone 1[12]) and 11.1 ± 2.0 cells/0.2 mm^2 in the pericentral areas (zone 3); the difference between the former and the latter was significant ($P < 0.05$). After GalN injection, the number of FSCs increased markedly in zone 1 and in the necrotic areas. On the 3rd day, the number of FSCs increased to 36.2 ± 7.0 cells/0.2 mm^2 and 30.9 ± 7.3 cells/0.2 mm^2 in zones 1 and 3, respectively, and, decreased to 19.6 ± 3.8 cells/0.2 mm^2 and 15.3 ± 3.2 cells/0.2 mm^2 in zones at 12 weeks, the number 1 and 3, respectively. The number of FSCs was greater in

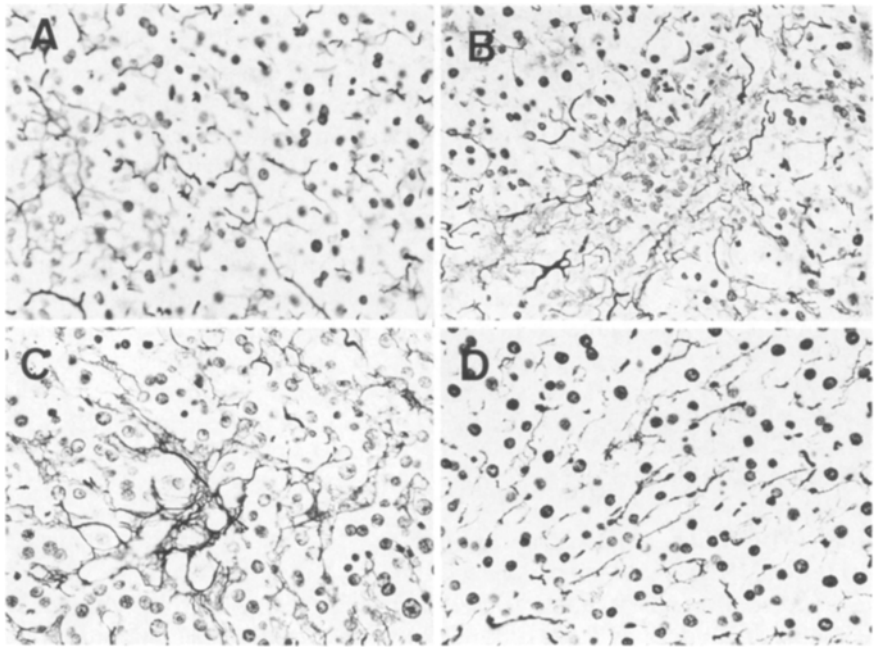

Fig. 2A–D. Alterations of the structure of reticular fibers in the lobules. **A** Normal structure of fibers in GalN-untreated rat liver. **B** Reticular fibers were not seen in the center of the necrotic area 2 days after GalN administration. **C** Bundles of fine reticular fibers appeared in and around the necrotic area 3 days after GalN administration. **D** The fiber structure returned to normal as late as 12 weeks after GalN administration. (Silver impregnation, ×100 orig. mag.)

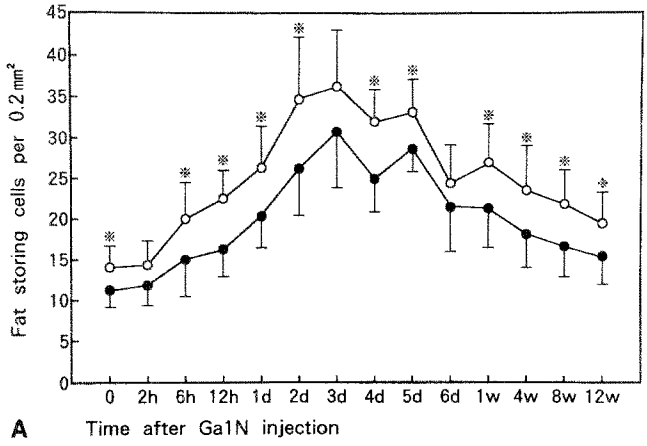

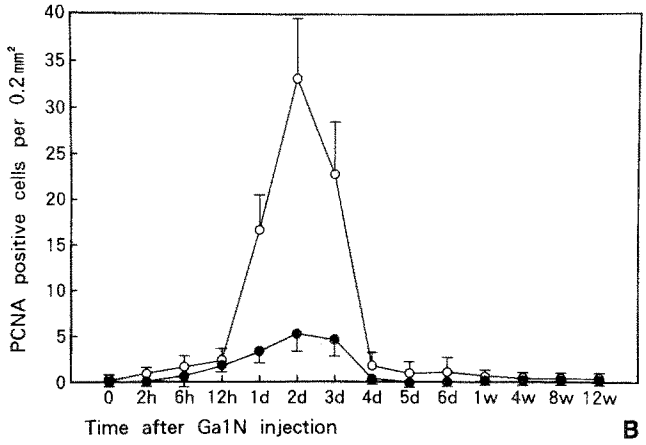

Fig. 3. **A** Changes in the number of fat-storing cells (*FSCs*) in periportal and pericentral areas. After GalN injection, the numbers of FSCs were significantly increased at 6 h and thereafter ($P < 0.05$), reaching their maximal values on the 3rd day in both the pericentral and periportal areas. The number of periportal FSCs (*circles*) was always greater than that of pericentral FSCs (*dots*). The data points represent the mean number of FSCs in nine periportal fields and nine pericentral fields of three sections (three sections per rat were examined and the counting was repeated in three rats) at each time point. *Vertical bars* indicate SD. *Significant difference ($P < 0.05$) between these two areas by Mann-Whitney test (two-tailed). **B** Changes in the numbers of proliferating cell nuclear antigen (*PCNA*) positively stained cells (hepatocytes and FSCs). The numbers of PCNA-positive hepatocytes and PCNA-positive FSCs increased significantly ($P < 0.05$) from 6 h to the 4th day and from 12 h to the 3rd day, respectively, reaching their maximal values on the 2nd day after GalN injection. The data points represent the mean number of total cells in nine periportal plus nine pericentral fields of three sections (one section per rat was examined and the counting was repeated in three rats) at each time point. *Vertical bars* indicate SD. *Circles*, PCNA-positive hepatocytes; *dots*, PCNA-positive FSCs

zone 1 than in zone 3 at all time points. To examine the proliferation of hepatocytes and FSCs after GalN injection, liver sections were double-stained for desmin and PCNA[13] (Fig. 4). PCNA-positive hepatocytes and PCNA-positive FSCs were more numerous in zone 1 than in zone 3. Figure 3B summarizes the numbers of PCNA-positive hepatocytes and PCNA-positive FSCs. In untreated rats, these values were 0.5 ± 0.5 cells/0.2 mm^2 and 0.2 ± 0.4 cells/0.2 mm^2, respectively. From 6 h to the 4th day and from 12 h to the 3rd day after GalN injection, these numbers were significantly increased ($P < 0.05$), respectively. Maximal values were observed on the 2nd day, when 33.0 ± 6.7 hepatocytes/0.2 mm^2 and 5.5 ± 2.1 FSCs/0.2 mm^2 were positive for PCNA.

Immunostaining of PGs in untreated liver

Immunoreactivity for each ECM component showed different localizations and different intensities in untreated rats. The intensity of immunostaining with antibodies 6B6, 1B5, 2B6, and 3B3 on chondrotinase ABC pretreatment and with HepSS-1 without chondroitinase ABC pretreatment is shown in Table 1 and Fig. 5. The interlobular bile duct and the reticular fibers in the lobules were not stained by 1B5 in GalN-untreated or treated rats, indicating no association of C-0S with these portions.

Expression of DS and HS after GalN injection

The intensity of immunostaining for DS decreased from the 2nd to the 6th day in portal tracts and from 12 h to the 6th day in lobular reticular fibers, and returned to normal 1 week after GalN injection. The changing profile of DS staining was similar to that of type III collagen. HS staining, which showed more complicated changes than the changes for other ECM components, decreased from 2 h to the 6th day and returned to the control level after 1 week in portal tracts, while increasing after 2 h to reach a peak on the 2nd day, followed by a decrease, in lobular reticular fibers. Some, but not all hepatocytes and the connective tissue in necrotic areas throughout the lobule were stained positively for HS from 12 h to the 2nd day. Sinusoidal walls, where HS was detected uniformly in Disse's space beneath the sinusoidal endothelia by TEM (data not shown), were stained weakly in zone 1 and the mid-zonal areas (zone 2), with the maximal intensity on the 2nd day after injection (Fig. 5).

Expression of C-0S, C-4S, and C-6S after GalN injection

Staining for C-0S, C-4S, and C-6S showed similar patterns, except that lobular reticular fibers and interlobular bile ducts were not stained for C-0S. In portal

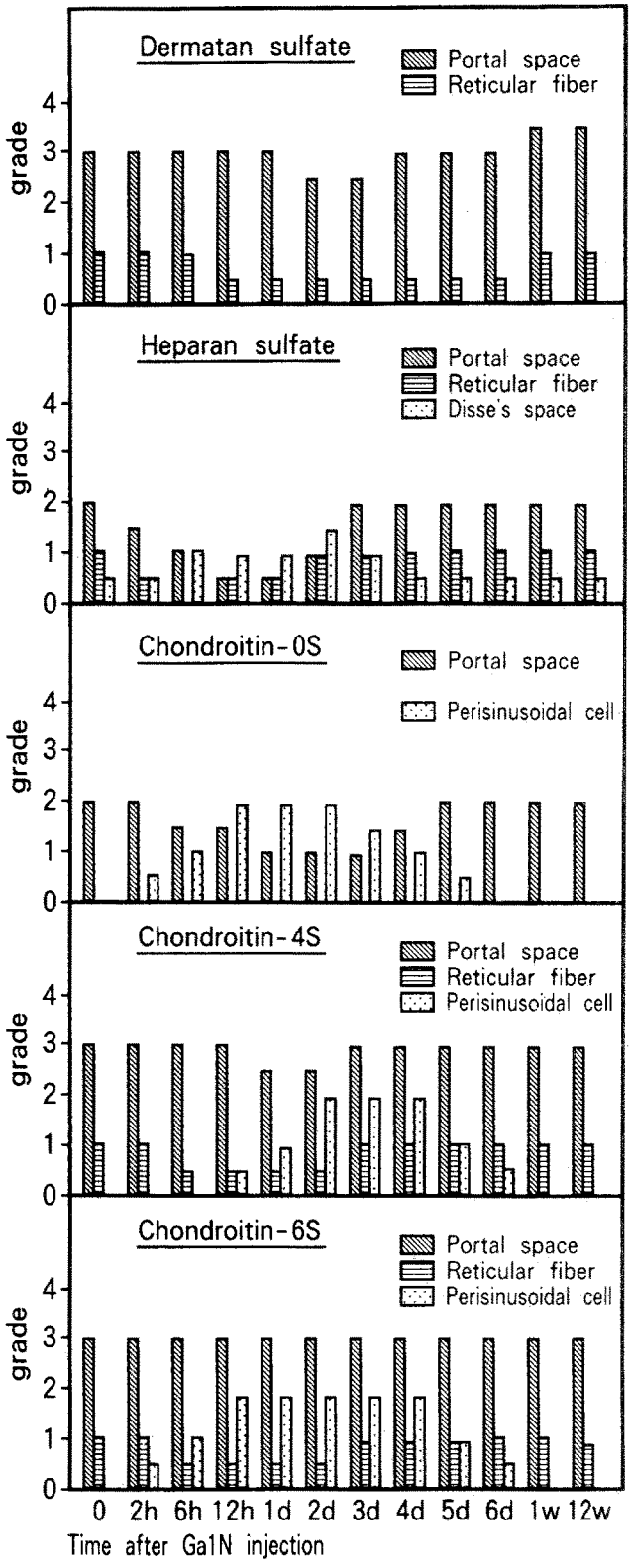

Fig. 5. Distribution of the staining for individual proteoglycans (*PGs*). The extent of immunoreactivity was graded semiquantitatively on a 0–4 scale. The *bars* represent the mean number of graded immunoreactivities. *0*, Absent; *1*, trace; *2*, weak; *3*, moderate; *4* strong

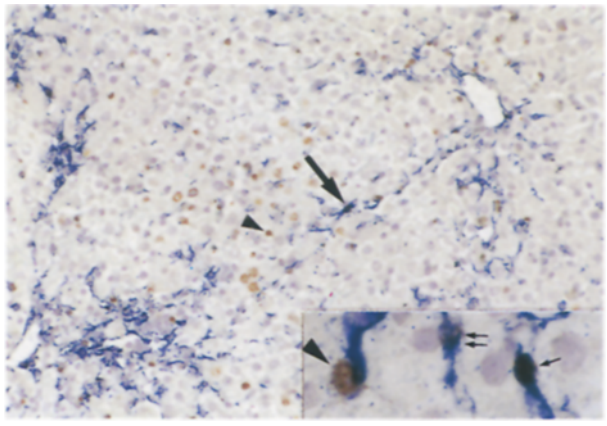

Fig. 4. Double-staining for desmin and PCNA in the rat liver on the 2nd day after GalN injection. 3-3′ Diaminobenzidine tetrahydrochloride (*DAB*) was used to visualize PCNA immunoreactivity (*brown*) and 4-methoxy-1-naphthol was used to visualize desmin immunoreactivity (*blue*) (×50, orig. mag.). *Inset*: Another field of a similar preparation showing a PCNA-positive hepatocyte (*arrowhead*), a PCNA-positive FSC (*arrow*), and a PCNA-negative FSC (*double arrow*). (×250, orig. mag.)

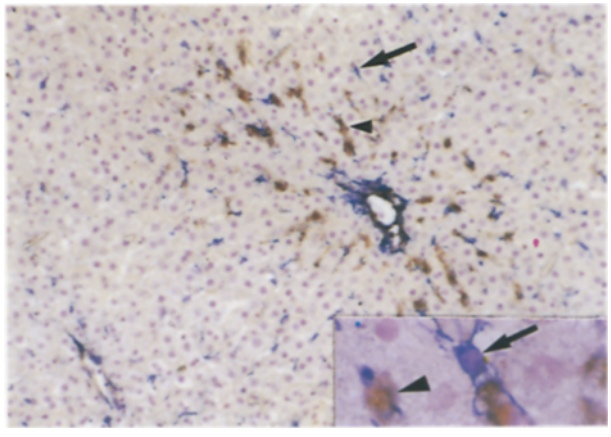

Fig. 6. Double staining for C-6S and desmin in the rat liver 12 h after GalN injection. Sinusoidal lining cells stained for C-6S (*arrowhead*), radiating from a portal tract, were co-located with desmin-positive FSCs (*arrow*) and were never costained for desmin. These chondroitin/chondroitin sulfate positive cells were more numerous in zone 1 than in zone 3, and were identical to sinusoidal endothelial cells. DAB and 4-methoxy-1-naphthol were used to visualize C-6S (*brown*) and desmin (*blue*) immunoreactivities, respectively (×50, orig. mag.). *Inset*: Another field of a similar preparation showing that C-6S-positive sinusoidal endothelial cells (*arrowhead*) were distinct from FSCs (*arrow*). (×250, orig. mag.)

Table 1. Immunoreactivity of individual ECM components in normal rat liver

	DS	HS	C-0S	C-4S	C-6S
Portal space					
Connective tissue fiber	+++	++	++	+++	+++
Interlobular vein	++++	+	++	++	+++
Interlobular artery	++++[a]	+	++	++	++
Interlobular bile duct	+++[b]	+	−	+	+
Lobule					
Hepatocyte	−	+[c]	−	−	−
Sinusoid (Disse's space)	−	+[d]	−	−	−
Reticular fiber	+	+	−	+	+
Central vein	++++	++	++	+++	+++

ECM, Extracellular matrix; *DS*, dermatan sulfate; *HS*, heparan sulfate; *C-0S*, chondroitin; *C-4S*, chondroitin 4-sulfate; *C-6S*, chondroitin 6-sulfate; −, absent; +, trace; ++, weak; +++, moderate; ++++, strong

[a] Tunica intima was not stained, but tunica media was stained

[b] Basal side of the epithelium was stained

[c] Some, but not all, hypatocytes were stained

[d] Stained in periportal areas

tracts, C-0S staining decreased from 6 h to the 4th day and C-4S staining decreased from the 1st to the 2nd day and thereafter returned to the control level, but the C-6S staining pattern showed no significant change after GalN injection. In the lobular reticular fibers, C-4S and C-6S staining, both of which were positive in untreated rat livers, decreased from 6 h to the 2nd day and returned to the control level after the 3rd day, while no staining for C-0S was observed at any time point after GalN injection. Sinusoidal lining cells, which were not stained in control rats, stained positively for C-0S, C-4S, and C-6S from 2 h to 1 week after GalN injection, radiating from the portal tracts, in zone 1 and zone 2, and these positively stained cells showed a distribution pattern similar to that of desmin-positive cells (Figs. 5, 6). By TEM, C-0S, C-4S, and C-6S were detected on the endoplasmic reticulum (ER) of non-parenchymal cells and in the connective tissue around these cells in necrotic areas at 6 h (Fig. 7A), and were further detected on the ER, the Golgi apparatus, and the cell membrane of sinusoidal endothelial cells from 6 h to the 2nd day after GalN injection (Fig. 7B); they were not detected on these portions of sinusoidal endothelial cells in negative control sections (Fig. 7C). Therefore, it appears that these non-parenchymal cells may synthesize C-0S/chondroitin sulfate (CS) PGs for this period of time.

Discussion

The present study was undertaken to investigate the time-related distribution of ECM component expression, focusing on PGs and the proliferation profiles of FSCs and hepatocytes, during liver injury and regeneration in rats induced by the administration of GalN. Liver injury in rats provoked by GalN administered by a variety of routes has many features in common with human viral hepatitis, and a well-reproducible dose-effect relationship is obtained if strains of rats of the same age and weight are used.[14] During this study, however, liver injury tended to be more severe in weak looking or dying rats than liver injury in other rats when they were killed. Consequently, excessively affected livers were not examined at each of the investigated time points. In control rat livers, the number of FSCs per 0.2 mm^2 was 26.1% higher in periportal than in pericentral areas. In the acute GalN models, the number of FSCs was increased between 6 h and 12 weeks, with a maximum on the 3rd day after injection both in the periportal and the pericentral areas, and these cells were always more numerous in the periportal than in the pericentral areas. Geerts et al.[11] reported that the number of FSCs increased in pericentral areas and did not alter in periportal areas after a single CCl_4 injection in rats.[11] In general, the experimental necrosis produced by GalN is diffuse rather than zonal, while that induced by CCl_4 is centrizonal.[15] Therefore, the number of FSCs may be increased in the damaged regions of the lobules, depending on the toxic agent applied. The number of PCNA-positive FSCs was significantly increased between 12 h and the 3rd day, and the maximal number was observed on the 2nd day after injection, when a 4.5-fold increase relative to control rats was observed. Many of the PCNA-positive FSCs were observed in clusters in necrotic areas, in contrast to the diffuse distribution of PCNA-positive hepatocytes throughout the lobules. These observations support the possibility of a direct paracrine flux of FSC

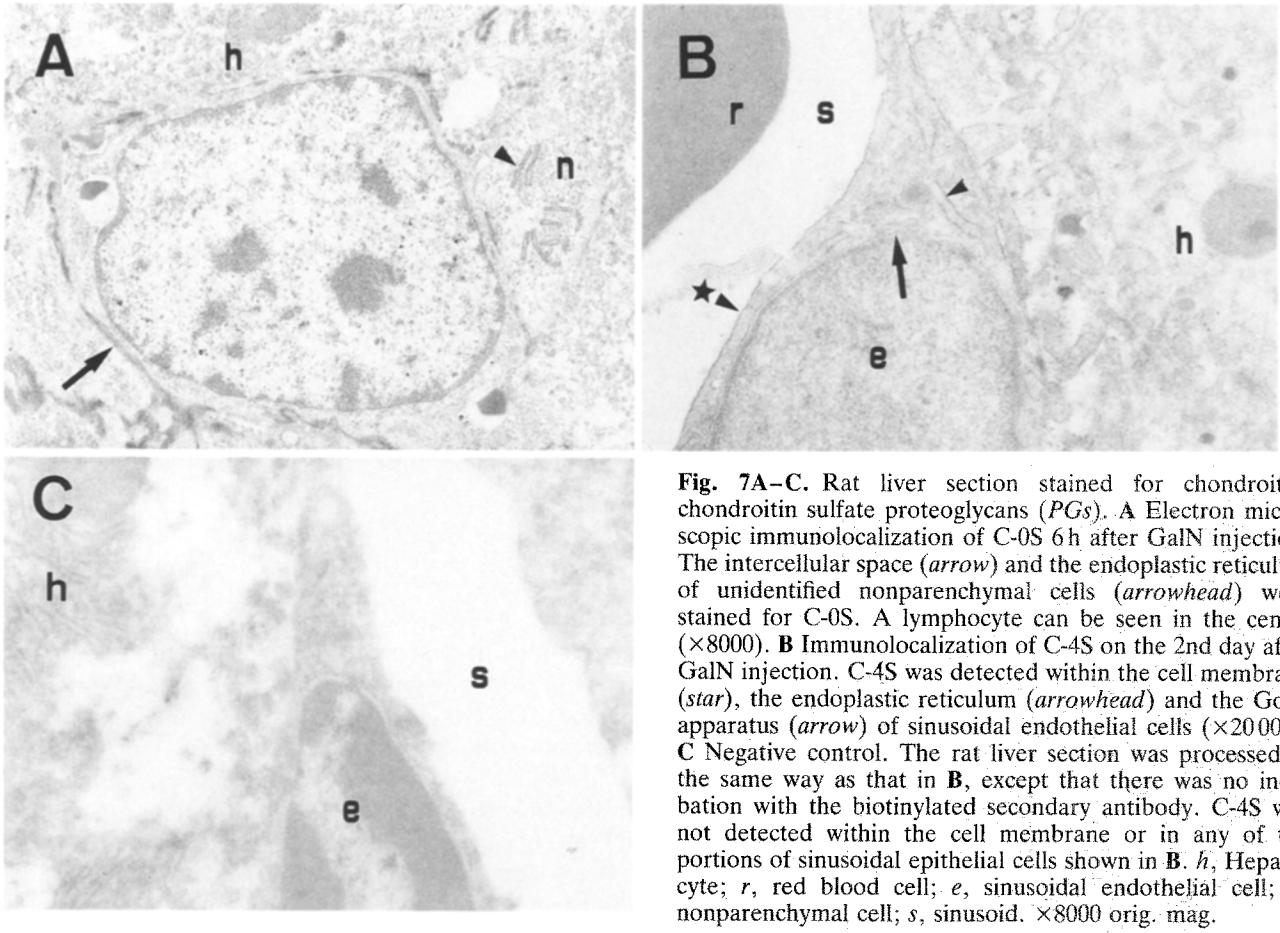

Fig. 7A–C. Rat liver section stained for chondroitin/chondroitin sulfate proteoglycans (*PGs*). **A** Electron microscopic immunolocalization of C-0S 6 h after GalN injection. The intercellular space (*arrow*) and the endoplastic reticulum of unidentified nonparenchymal cells (*arrowhead*) were stained for C-0S. A lymphocyte can be seen in the center (×8000). **B** Immunolocalization of C-4S on the 2nd day after GalN injection. C-4S was detected within the cell membrane (*star*), the endoplastic reticulum (*arrowhead*) and the Golgi apparatus (*arrow*) of sinusoidal endothelial cells (×20000). **C** Negative control. The rat liver section was processed in the same way as that in **B**, except that there was no incubation with the biotinylated secondary antibody. C-4S was not detected within the cell membrane or in any of the portions of sinusoidal epithelial cells shown in **B**. *h*, Hepatocyte; *r*, red blood cell; *e*, sinusoidal endothelial cell; *n*, nonparenchymal cell; *s*, sinusoid. ×8000 orig. mag.

growth-promoting factor from damaged hepatocytes to FSCs.[16]

PGs consist of a protein core, which may be genetically distinct, and a variable number of glycosaminoglycans (GAGs) covalently linked to serine, threonine, or asparagine residues on the core.[17] Many PGs have been discovered and tentatively classified into categories:[18] extracellular matrix/basement membrane PGs,[19,20] membrane-intercalated/cell-surface PGs,[21–23] and intracellular PGs.[24] The predominant PGs in liver tissue are HS, DS, CS, and hyaluronic acid, which show not only several-fold increases in amount, but also histological redistribution of the constituents in fibrotic liver.[25]

In control rat liver, the immunostaining pattern for DSPG[7] was similar to that of type III collagen, rather than to that of type I collagen. After GalN injection, the intensity in the portal tracts decreased from the 2nd to the 3rd day, followed by an increase from 1 week; in the reticular fibers in the lobules, the intensity decreased from 12 h to the 6th day; and no DSPG staining was observed in the necrotic areas at any time point. The number of PCNA-positive hepatocytes showed a peak value on the 2nd day. These observations suggest that DSPG induces hepatocytes not to proliferate, but to differentiate, and to maintain their characteristic functions through interactions with cytokines, such as TGF-α and TGF-β, similar to the effect for FSCs.[25]

In this study, HS in untreated rat liver was detected in the portal space, reticular fibers, the sinusoidal wall, and the central vein by LM. From 2 h to the 1st day after GalN injection, the immunostaining intensity was decreased in the portal tracts and the reticular fibers. On the other hand, intensity was increased in Disse's space, and some, but not all, hepatocytes in the lobules were stained positively, in addition to extracellular spaces in the necrotic areas throughout the lobules, from 12 h to the 2nd day. The distribution of hepatocytes stained by HepSS-1 was consistent with that of PCNA-positive hepatocytes. These observations are in agreement with those of other reports.[26,27] It is likely that HepSS-1 detected some or all kinds of HSPG molecules. This may indicate that each component of the liver shows a different and complicated pattern of changing immunostaining intensity with HepSS-1.

Many PGs with CS-GAG side chains have been reported to date: extracellular aggrecan,[28] PG-M/

versican,[29] phosphacan;[30] cell-surface NG2;[31] intracellular PG,[24,32] and others. These CSPGs, as do HSPGs, have multiple functional properties. For instance, the migration efficiency of melanoma cells may be enhanced in the presence of TGF-β by additional mechanisms that act in combination with CD44-CSPG.[33] Phosphacan-CSPG, which represents the glycosylation and possible extracellular splicing variants of a receptor type protein tyrosine phosphatase, may modulate cell interaction and developmental processes.[30] It has been reported that FSCs are an important source of PG in normal liver,[34] and that they synthesize at a high rate in vitro all the noncollagenous matrix components occurring in the fibrotic liver matrix.[35] We found that C-0S, C-4S, and C-6S PGs were expressed in the sinusoidal lining cells in the periportal area from 2 h to the 6th day after GalN injection. These C-0S-, C-4S-, and C-6S-positive cells were colocalized with desmin-positive FSCs, and were never costained with anti-desmin antibody. By TEM, C-0S, C-4S, and C-6S PGs were detected at 12 h in necrotic areas uniformly around lymphocytes and nonparenchymal cells, the cell types of which were not determined. They were also detected within the cell membranes, the ER membranes, and the Golgi apparatus of the sinusoidal endothelial cells from 6 h to the 2nd day after GalN injection. These obsenvations suggest that C-0S/CS PGs are synthesized, at least transiently, by non-parenchymal cells including sinusoidal endothelia C-0S/CS PGs may play an important role in liver regeneration.

Acknowledgments. We thank Mr. S. Awai (Department of Pathology, Okayama University) and Dr. H. Matsushima and Mr. S. Inoue (Shigei Medical Research Institute) for their technical assistance. This work was supported by Grants from the Japanese Ministry of Education (No. 02807074, No. 04304038) and from the Japanese Ministry of Health and Welfare (No. 2-1-2).

References

1. Schuppan D. Structure of the extracellular matrix in normal and fibrotic liver: Collagens and glycoproteins. Semin Liver Dis 1990;10:1–10.
2. Martinez-Hernandez A, Amenta PS. Morphology, localization and origin of the hepatic extracellular matrix. In: Zern MA, Reid LM (eds) Extracellular matrix: Chemistry, biology, and pathobiology with emphasis on the liver. New York: Marcel Dekker, 1993;255–327.
3. Koide N, Sakaguchi K, Koide Y, et al. Formation of multicellular spheroids composed of adult rat hepatocytes in dishes with positively charged surfaces and under other nonadherent environments. Exp Cell Res 1990;186:227–235.
4. Murata K, Ochiai Y, Akashio K. Polydispersity of acidic glycosaminoglycan components in human liver and the changes at different stages in liver cirrhosis. Gastroenterol 1985;89:1248–1257.
5. Jezequel AM, Ballardini G, Mancini R, et al. Modulation of extracellular matrix components during dimethylnitrososamine-induced cirrhosis. J Hepatology 1990;11:206–214.
6. Kure S, Yoshie O. A syngeneic monoclonal antibody to murine meth-A sarcoma (HepSS-1) recognizes heparan sulfate glycosaminoglycan (HS-GAG): Cell density and transformation-dependent alteration in cell surface HS-GAG defined by HepSS-1. J Immunol 1986;137:3900–3908.
7. Sobue M, Nakashima N, Fukatsu T, et al. Production and characterization of monoclonal antibody to dermatan sulfate proteoglycan. J Histochem Cytochem 1988;36:479–485.
8. Poole AR, Webber C, Pidoux I, et al. Localization of a dermatan sulfate proteoglycan (DS-PGII) in cartilage and the presence of an immunologically related species in other tissues. J Histochem Cytochem 1986;34:619–625.
9. Couchman JR, Caterson B, Christner JE, Baker JR. Mapping by monoclonal antibody detection of glycosaminoglycans in connective tissues. Nature 1984;307:650–652.
10. Callea F, Mebis J, Desmet VJ. Myofibroblasts in focal nodular hyperplasia of the liver. Virchows Arch [A] 1982;396:155–166.
11. Geerts A, Lazou JM, Bleser de P, et al. Tissue distribution, quantitation, and proliferation kinetics of fat-storing cells in carbon tetrachloride-injured rat liver. Hepatology 1991;13:1193–1202.
12. Matsumoto T, Komori R, Magara T, et al. A study on the normal structure of the human liver, with special reference to its angioarchitecture (in Japanese with English abstract). Kanzo (Acta Hepatol Jpn) 1979;20:223–247.
13. Prelich G, Kostura M, Marshak DR, et al. The cell-cycle regulated proliferating cell nuclear antigen is required for SV40 DNA replication in vitro. Nature 1987;325:471–475.
14. Decker K, Keppler D. Galactosamine-induced liver injury. In: Popper HP, Schaffner F (eds) Progress in liver diseases. Vol 4. New York: Grune and Stratton, 1972;183–199.
15. Zimmerman HJ, Maddrey WC. Toxic and drug-induced hepatitis. In: Schiff L, Schiff ER (eds) Diseases of the liver. 6th Ed. Philadelphia: J.B. Lippincott, 1987;591–667.
16. Gressner AM, Lotfi S, Gressner G, et al. Identification and partial characterization of a hepatocyte-derived factor promoting proliferation of cultured fat-storing cells (parasinusoidal lipocytes). Hepatology 1992;16:1250–1266.
17. Kjellén L, Lindahl U. Proteoglycans: Structures and interactions. Annu Rev Biochem 1991;60:443–475.
18. Rouslahti E. Structure and biology of proteoglycans. Ann Rev Cell Biol 1988;4:229–255.
19. Soroka CL, Farquhar MC. Characterization of a novel heparan sulfate proteoglycan found in the extracellular matrix of liver sinusoids and basement membranes. J Cell Biol 1991;113:1231–1241.
20. Noonan DM, Fulle A, Valente P, et al. The complete sequence of perlecan, a basement membrane heparan sulfate proteoglycan, reveals extensive similarity with laminine A chain, low density lipoprotein-receptor, and the neural cell adhesion molecule. J Biol Chem 1991;266:22939–22947.
21. Bernfield M, Kokenyesi R, Kato M, et al. Biology of the syndecans: A family of transmembrane heparan sulfate proteoglycans. Annu Rev Cell Biol 1992;8:365–393.
22. Karthikeyan L, Maurel P, Rauch U, et al. Cloning of a major heparan sulfate proteoglycan from brain and identification as the rat form of glypican. Biochem Biophys Res Commun 1992;188:395–401.
23. David G, B van der Schueren, Marynen P, Cassiman JJ, et al. Molecular cloning of amphyglycan, a novel integral membrane heparan sulfate proteoglycan expressed by epithelial and fibroblastic cells. J Cell Biol 1992;118:961–969.
24. Bourdon MA, Oldberg Å, Pierschbacher M, et al. Molecular cloning and sequence analysis of a chondroitin sulfate proteoglycan cDNA. Proc Natl Acad Sci USA 1985;82:1321–1325.

25. Meyer DH, Krull N, Dreher KL, et al. Biglycan and decorin gene expression in normal and fibrotic rat liver: Cellular localization and regulatory factors. Hepatology 1992;16:204–216.
26. Gressner AM, Pfeiffer T. Preventive effects of acute inflammation on liver cell necrosis and inhibition of heparan sulfate synthesis in hepatocytes. J Clin Chem Clin Biochem 1986;24: 821–829.
27. Preston SF, Regula PR, Sager CB, et al. Glycosaminoglycan synthesis is depressed during mitosis and elevated during early Gl. J Cell Biol 1985;101:1086–1093.
28. Doege KJ, Sasaki M, Kimura T, et al. Complete coding sequence and deduced primary structure of the human cartilage large aggregating proteoglycan, aggrecan. J Biol Chem 1991; 266:894–902.
29. Yamagata M, Suzuki S, Akiyama SK, et al. Chondroitin sulfate proteoglycan (PG-M-like proteoglycan) is involved in the binding of hyaluronic acid to cellular fibronectin. J Biol Chem 1986; 261:13526–13535.
30. Maurel P, Rauch U, Flad M, et al. Phosphacan, a chondroitin sulfate proteoglycan of brain that interacts with neurons and neural cell-adhesion molecules, is an extracellular variant of a receptor-type protein tyrosine phosphatase. Proc Natl Acad Sci USA 1994;91:2512–2516.
31. Nishiyama A, Dahlin KJ, Prince JT, et al. The primary structure of NG2, a novel membrane-spanning proteoglycan. J Cell Biol 1991;114:359–371.
32. Lohmander LS, Arnljots K, Yanagisita M. Structure and synthesis of intracellular proteoglycan in HL-60 human leukemic promyelocytes. J Biol Chem 1990;265:5802–5808.
33. Faassen AE, Mooradian DL, Tranquillo RT, et al. Cell surface CD44-related chondroitin sulfate proteoglycan is required for transforming growth factor-β-stimulated mouse melanoma cell motility and invasive behavior on type I collagen. J Cell Sci 1993;105:501–511.
34. Arenson DM, Friedman SL, Bissell DM. Formation of extracellular matrix in normal rat liver: Lipocytes as a major source of proteoglycan. Gastroenterology 1988;95:441–447.
35. Gressner AM, Bachem MG. Cellular sources of noncollagenous matrix proteins: Role of fat-storing cells in fibrogenesis. Semin Liv Dis 1990;10:30–46.